Application of Machine-Learning for the Prediction of Formation Rate of Silica Scale from Geothermal Water

Saefudin Juhri[1], Kotaro Yonezu[1], Terashi Ryunosuke[1], Katsuki Manaya[1], Eiki Watanabe[2], Koichiro Mori[2], Shogo Sato[2], Naho Inoue[2], Haryo Edi Wibowo[3], Takushi Yokoyama[2,4]

[1] Dept. Earth Resources Engineering, Kyushu University, Fukuoka, Japan

[2] Kyudensangyo Co., Inc., Fukuoka, Japan

[3] Dept. Geological Engineering, Universitas Gadjah Mada, Yogyakarta, Indonesia

[4] Dept. Chemistry, Kyushu University, Fukuoka, Japan

juhri@mine.kyushu-u.ac.id

Keywords: *machine learning, artificial intelligence, silica, scaling, geothermal*

ABSTRACT

Utilization and development of geothermal energy are still hindered by scaling and corrosion to this day. Scaling is particularly troublesome as it can occur in almost all locations in geothermal power plants, i.e., in production wells, on surface facilities, in reinjection wells, and even in the reservoir rock formation around the reinjection wells. However, there is no single and universally applicable mitigation method to date, due to the unique characteristics of each geothermal water and the complexity of scale formation. This study aims to better understand and quantify silica scaling assisted by artificial intelligence (AI), i.e., supervised machine learning (SML).

The SML was used to predict the formation rate of silica scale based on the physicochemical characteristics of geothermal water and the kinetics of polymerization of silicic acid in geothermal water and adsorption of silicic acid on the surface of scale substances. These data were used as input parameters in the training data. The data was obtained from onsite batch experiments in several geothermal power plants in Japan. The rate of silica scale formation from onsite plate immersion experiments using stainless-steel plate was used as the output parameters. This experiment was conducted for up to 5 hours in the corresponding geothermal power plants.

The produced models are evaluated based on their percent relative root means squared error (%RRMSE) value when used to predict unknown data, i.e., non-training data. Our study showed that the model can achieve %RRMSE value of 15 which is in the good category, i.e., the model can accurately predict the formation rate of silica scale within 5 hours. Furthermore, the model will be trained to predict the formation rate of silica scale for up to 5 days and beyond. This study is expected to aid geothermal power plants to mitigate the silica scale problem more efficiently.

1. INTRODUCTION

Scaling and corrosion remain the most common challenges in the utilization and development of geothermal energy. Scaling is particularly more troublesome as it can occur in almost all surface and subsurface facilities. Calcite scale may occur due to the boiling of geothermal fluid at high temperature within the production well (Wanner et al., 2017). Sulfide scale might form in the two-phase pipeline (e.g., Jamero et al., 2018 and Juhri et al., 2023). In addition, sulfur scale has also been reported to affect the cooling tower (Kudo & Yano, 2000; Relenyi & Rosser, 2016; Rodriguez, 2023) and heat exchanger (Garcia et al., 2002) of geothermal power plants. Furthermore, silica can precipitate due to steam separation and decrease in temperature inside the separator and brine pipeline. Finally, silica can also precipitate within the pores of reservoir rock (Yanaze et al., 2016), decreasing the productivity of the geothermal reservoir. All of these instances can significantly hinder energy production from geothermal power plants.

Among the many types of scale, silica scale might form in almost all locations. Therefore, there has been excessive studies on silica scale. The current general understanding on silica scale formation suggests that there are two pathways of scale initiation: interaction between dissolved silicic acid and the surface of the pipeline (heterogenous nucleation) and interaction among dissolved silicic acid to form silica particles (homogenous nucleation) (Rothbaum et al., 1979; Chan, 1989; Gallup and Reiff, 1991; Yokoyama et al., 1993; Mi & Elimelech, 2013). Furthermore, silica scale grows further owing to the interaction between dissolved silicic acid in geothermal water and the surface of silica scale.

Despite the vast studies on silica scaling, there has not been a universally applicable mitigation method for this problem. This is due to the various factors that can control the rate of interaction between dissolved silicic acid in geothermal water. Among those factors are the salinity of geothermal water, pH, metal contents (e.g., Al, Fe, and Mg), temperature, and fluoride content (Tarutani, 1989; Yokoyama et al., 1993; Manceau et al., 1995; and Gallup et al., 1997). Finding a universally applicable prevention method becomes more complicated due to the unique characteristics of geothermal water in each field and, consequently, the complexity of scale formation mechanism.

Recently, artificial intelligence (AI) has been applied in many fields of scientific research to assist the research strategy and modelling. In particular, AI is being used in the geothermal energy exploration such as estimating the reservoir temperature, determining the production drilling, and development of enhance geothermal system (e.g., Al Shibli and Mathew, 2019; Shahdi, et al., 2021; Moraga et al., 2022; Wang et al., 2023). In this study, we attempt to utilize artificial intelligence, in particular machine-learning, to better understand and quantify silica scaling. The supervised machine-learning (SML) was tasked to predict the formation rate of silica scale based on the empirical data of physicochemical properties of geothermal water responsible for the scale formation. In addition, due to the nature of interaction among dissolved silicic acid, the experimental data of the kinetics behavior of the polymerization and adsorption of dissolved silicic acid were also studied and taken into consideration. The prediction model from this study was expected to be accurate and adaptive for further improvement with more experimental data in the future.

2. METHODOLOGY

2.1 Physicochemical Properties of Geothermal Water

The physicochemical properties of the geothermal water consist of pH, concentrations of major anions and cations, and concentrations of total silicic acid (Si-T), monosilicic acid (Si-M), and metals (Fe, Al, Mg). The pH and concentration of monosilicic acid were analyzed onsite at geothermal power plants, whereas concentration of total silicic acid and metals were analyzed at Economic Geology Laboratory, Kyushu University. In addition, major ions data were obtained from the operator of the geothermal power plants. These data were used in the training data for the supervised machine-learning as input parameters.

2.2 Onsite Polymerization and Adsorption Experiment

In addition to the physicochemical data of geothermal water, the kinetics of silicic acid polymerization and its adsorption on silica gel were also studied and introduced in the training data. Therefore, onsite experiments were conducted in several geothermal power plants in Japan. Both experiments were conducted in the temperature range of 90 – 95 °C. Prior to the analysis, samples from both experiments were filtered by 0.45 μm membrane, and immediately acidified with nitric acid.

Polymerization experiments of silicic acid were conducted for 60 minutes where an adequate amount of geothermal water was sampled every 5 – 15 minutes. From these samples, the concentration of monosilicic acid (Si-M) was determined on-site by spectrophotometric analysis while total concentration of silicic acid (Si-T) was determined in laboratory by ICP-AES. The behavior of silicic acid polymerization was observed from the change of their concentrations during the experiment.

Furthermore, adsorption experiments of silicic acid on silica gel (D-50-1000AW) were conducted to observe the interaction between dissolved silicic acid with the surface of silica gel which represent the surface of pre-formed silica scale. The specific surface area of the silica gel was known to be 28 m^2/g. The adsorption behavior of silicic acid was expressed as the decrease of total silicic acid concentration after considering the effect of its polymerization.

2.3 Onsite Plates Immersion Experiment

Plates immersion experiments were conducted to quantify the rate of silica precipitation on the surface of solid material for a short period of time. In this study, stainless steel plates were immersed in geothermal water corresponding to the polymerization and adsorption experiments, for 5 hours period and 5 days period. A piece of plate was lifted every one hour and one day, respectively. The plate samples were rinsed with ultrapure water and ethanol to ensure brine-free sample and avoid further reaction.

Plate samples were analyzed by laser ablation coupled with ICPMS to detect silica content on the plates' surface at ppm level. The increase of Si content on plate samples was translated to precipitation rate of silica scale on plate surface and used as the output parameter of the training data for machine-learning.

2.4 Machine Learning Architecture

The Dense Feed-forward Neural Network (DFFN) supervised machine-learning architectures were examined in this study. The architecture consists of an input layer with 21 features, x-number of hidden layers with y-number of neuron units each, and an output layer with 1 feature. The x and y ranges from 1 – 10 and 1 – 100, respectively. The input for each hidden layer passed through a batch normalization layer for smooth learning process. In this study, the neuron units in the hidden layers were activated using the ReLU function.

2.4.1 Range of training data

The training data in this study consists of a wide range of characteristics. The salinity (wt % NaCl equivalent) of the geothermal water ranges from 2,540 to 29,973 while the pH ranges from 4.0 to 9.0. This means the model built from this training data encompasses dilute to saline and acidic to alkaline geothermal waters. Furthermore, the concentrations of Si-T(0), Fe-T, and Al-T ranges from 388 to 993, <0.01 to 0.8, and <0.01 to 0.9, respectively. This further signifies the model's applicability to predict the silica scaling from various types of geothermal water.

2.4.2 Preprocessing

The training data (input and output parameters) were preprocessed before used for AI training. All input parameters (physicochemical properties and kinetics behavior of silicic acid) were normalized using minimum-maximum method. Furthermore, the output parameter was also normalized using minimum-maximum method.

2.4.3 Model evaluation

The accuracy of the prediction was quantified based on the value of root mean square error in percent scale (Despotovic et al., 2016). The value of RMSE was calculated using the equation 1 below, where $H_{i,m}$ is measured data from onsite experiments and $H_{i,c}$ is calculated data by AI model. From this RMSE value, the models are categorized into excellent (<10%), good (10-20%), fair (20-30%), and poor (>30%) (Jamieson et al., 1991; Heinemann and Schmidhalter, 2012; Li et al., 2013).

$$\%RMSE = \frac{\sqrt{\frac{1}{n}\sum_{i=1}^{n}\left(H_{i,m}-H_{i,c}\right)^2}}{\frac{1}{n}\sum_{i=1}^{n}H_{i,m}} \times 100 \quad \text{……….} (1)$$

3. RESULTS AND DISCUSSION

3.1 Model Accuracy

The accuracy of the machine-learning models was evaluated based on their ability to predict the precipitation rate of Si on metal plates. Four experiments at four different geothermal power plants were used to evaluate the prediction accuracy. The general characteristics of the geothermal waters are tabulated in Table 1 whereas the polymerization and adsorption behavior of silicic acid is depicted in Figure 1.

Table 1. General characteristics of the geothermal waters (GW) used as evaluation data.

GW	pH	Na	K	Ca	Cl	Si-T	Si M / Si T	Al-T	Fe-T
a	7.60	1,440	229	11	2,540	894	0.800	0.5	0.80
b	5.09	9,236	1,229	1,569	19,056	624	0.992	0.08	0.19
c	7.26	9,878	1,290	1,682	20,095	704	0.917	0.02	0.46
d	6.45	4,070	499	573	8,128	388	0.997	0.04	0.05

Figure 2 shows the prediction of the Si precipitation rate on metal plates based on DFFN architecture compared to the experimental value from each corresponding geothermal water. The best model was attained with 4 hidden layers each containing 64 neuron units. This model has an R^2 value of 0.987 and an RRMSE value of 12.6% (Figure 3) which is categorized as a good model. The model can accurately predict the precipitation rate of Si on metal plates immersed in geothermal water for up to 5 days.

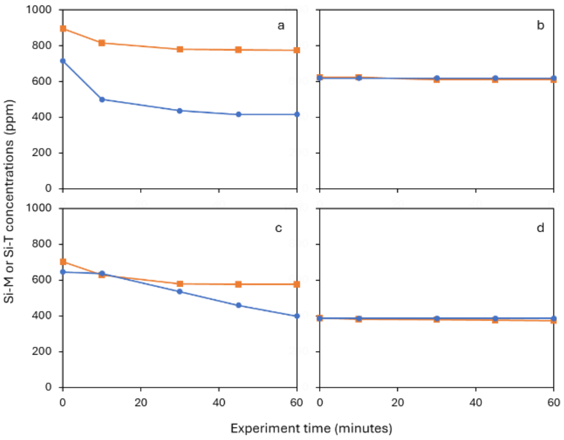

Figure 1: Polymerization and adsorption behavior of silicic acid in four geothermal waters from four geothermal power plants

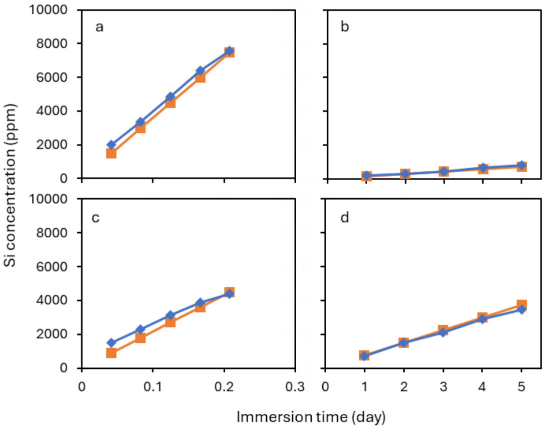

Figure 2: Comparison between Si concentration values from onsite experiment and DFFN model's prediction of 4 geothermal waters with different characteristics.

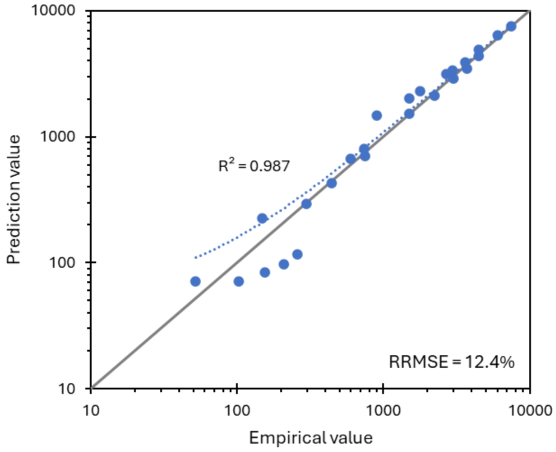

Figure 3: Statistical evaluation of the DFFN model.

3.2 Long-Term Prediction

Furthermore, the model can accurately predict the precipitation of Si on metal plates up to 35 days with a clear distinction between near neutral geothermal water (a & c) and acidic geothermal waters (b & d), as seen in Figure 4. The prediction from the model indicates that at near neutral pH, the early precipitation of silica scale (within 5 hours) was substantially faster than at acidic pH. This is in agreement with the previous studies on the effect of pH to the interaction among dissolved silicic acids and between silicic acid with the surface of silica particles (Tarutani, 1989 and references therein). Further, the precipitation of Si seems to follow a linear function through time. On the other hand, the precipitation rate of Si at acidic pH was significantly slower than that of near neutral pH within the first 5 days of immersion time.

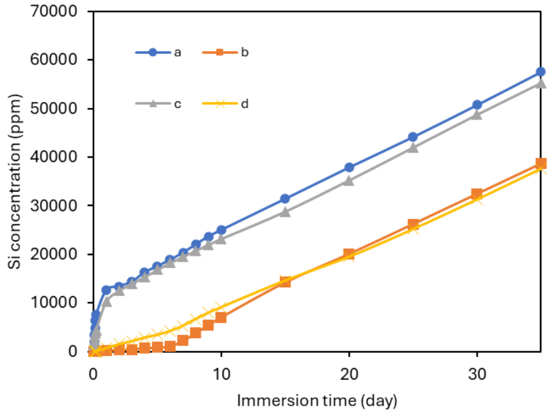

Figure 4: Long-term prediction of Si precipitation on metal plates from 4 different geothermal waters.

3.3 Factor Analysis

Based on the experimental data and the prediction of the precipitation of Si on metal plates, the most distinct precipitation behavior occurs at the early stage of Si precipitation (5 hours immersion time). Therefore, contribution factor analysis was carried out to determine parameter that contribute to the precipitation of Si during up to 5 hours of immersion time.

As seen from Figure 5, the main parameters that contribute positively to the precipitation of Si are the ratio of monosilicic acid over the total silicic acid (Si-M/Si-T) at initial conditions, total concentration of dissolved silicic acid (Si-T), chloride, aluminum, and pH of the geothermal water. This is in line with the previous experimental studies (e.g., Marshall & Warakomski, 1980; Tarutani, 1989; Yokoyama et al., 1989; Gallup, 1997). These parameters contribute 6.4%, 5.6%, 5.1%, 3.8%, and 3.4%, respectively. On the contrary, the polymerization rate of dissolved silicic acid and its adsorption on silica gel generally contribute negatively to the precipitation of Si at the early stage. Result of the contribution factor analysis for the precipitation of Si within 5 hours suggests that the initiation of Si precipitation is mainly controlled by the degree of silica polymerization at initial stage (Si-M/Si-T), total concentration of dissolved silicic acid, concentrations of chloride and aluminum, as well as the pH of geothermal water.

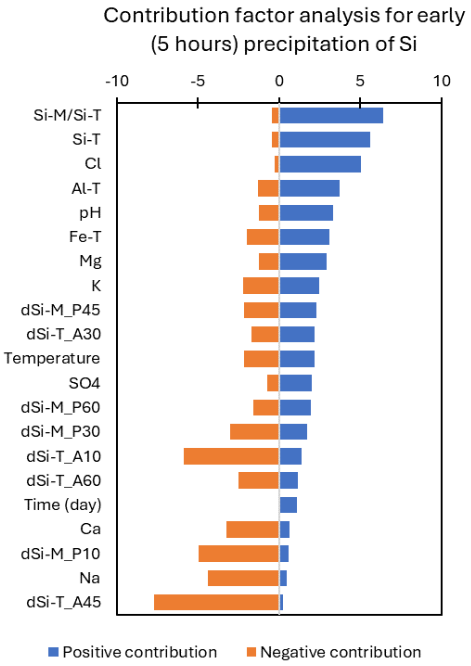

Figure 5: Contribution factor of input parameters (major characteristics of geothermal water and kinetics behavior of dissolved silicic acid) to the precipitation of Si on the metal plates within 5 hours of experimental.

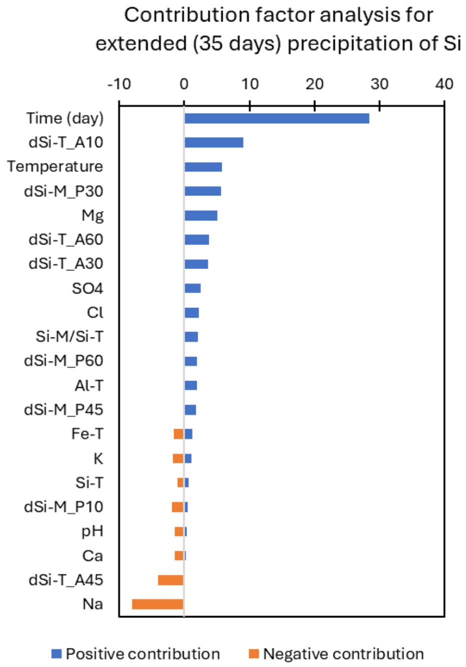

Figure 6: Contribution factor of input parameters (major characteristics of geothermal water and kinetics behavior of dissolved silicic acid) to the precipitation of Si on the metal plates from day 5 to day 35 of the immersion experiment.

Furthermore, contribution factor analysis was also conducted for the extended precipitation of Si (beyond 5 days) in order to understand parameters that control the growth of the silica scale. As depicted in Figure 6, other than experimental time, the main contributing factors are adsorption rate of dissolved silicic acid, temperature, and polymerization rate of silicic acid. This is in accordance with the current understanding that interaction between dissolved silicic acid and the surface of silica scale (i.e., adsorption of dissolved silicic acid) control the growth of the silica scale (Juhri et al., 2024).

4. CONCLUSION AND IMPLICATION

This study provides a steppingstone towards the universal prediction of silica scale formation. With the low RRMSE value of 12.6%, the model is considered accurate in predicting the precipitation of silica on metal plates. Furthermore, the constructed model is possible to be updated with future onsite experiments, owing to its flexible and adaptive behaviour.

In addition, the contribution factor analyses showed that different parameters control the initiation and the growth of silica scale. The initiation of silica scale formation was likely controlled by the ratio of monosilicic acid over total silicic acid at initial conditions, the concentrations of total silicic acid, levels of chloride, iron and aluminium ions present, as well as the pH of geothermal water. On the contrary, the growth of the silica scale was mainly controlled by the kinetic behaviour of dissolved silicic acid, i.e. polymerization and adsorption behaviour, and temperature of the geothermal water. This analysis result could open a possibility of developing a universal prevention method for silica scale problem in geothermal power plant.

ACKNOWLEDGEMENTS

This work was financially supported by the New Energy and Industrial Technology Development Organization's (NEDO) project (2021–2025): Research and development of geothermal energy generation technology / Development of technology for advanced use of geothermal energy / Developments of the scale monitoring method for improvement of operation efficiency of power generation facilities and utilization technology of AI.

REFERENCES

Al Shibli, M., and Mathew, B. (2019). Artificial Intelligent Machine Learning and Big Data Mining of Desert Geothermal Heat Pump: Analysis, Design and Control, International Journal of Intelligent Systems and Applications, 10(4), 1-13.

Chan, S.H., (1989). A review on solubility and polymerization of silica. Geothermics 18 (1- 2), 49–56.

Despotovic, M., Nedic, V., Despotovic, D., and Cvetanovic, S. (2016). Evaluation of empirical models for predicting monthly mean horizontal diffuse solar radiation, Renewable and Sustainable Energy Reviews, 56, 246-260.

Gallup, D. L. (1997). Aluminum silicate scale formation and inhibition: scale characterization and laboratory experiments. Geothermics, 26(4), 483-499.

Gallup, D.L., and Reiff, W.M., (1991). Characterization of geothermal scale deposits by Fe-57 Mossbauer spectroscopy and complementary X-ray diffraction and infra-red studies. Geothermics 20 (4), 207–224.

Garcia, T.G.G., Manila, J.G., Nanual, N.A., and Ho, P. (2002). An Innovative Approach to Mitigating Sulfur Deposition in The Condenser at Mahanagdong Geothermal Power Plant. In: Proceedings of 23rd Annual PNOC-EDC Geothermal Conference. Makati, Philippines. March, 2002.

Heinemann, P., and Schmidhalter, U. (2022). Spectral assessments of N-related maize traits: Evaluating and defining agronomic relevant detection limits, Field Crops Research, 289, 108710.

Jamero, J.L., Monterozo, F.E.P., Gill, J.S., and Salidaga, J.A., (2021). Mitigation of two-phase header scaling in an acidic system. In: Proceedings of the World Geothermal Congress 2020+1. Reykjavik, Iceland. April - October 2021.

Jamieson, P.D., Porter, J.R., and Wilson, D.R. (1991). A test of the computer simulation model ARCWHEAT1 on wheat crops grown in New Zealand. Field crops research, 27(4), 337-350.

Juhri, S., Yonezu, K., Harijoko, A., Nurpratama, M. I., and Yokoyama, T. (2023). Diverse scale deposition in response to the change in chemical properties of geothermal water at the Dieng geothermal power plant, Indonesia. Geothermics, 111, 102717.

Kudo, S., and Yano, T. Sulfur Scale Abatement System Using a Surfactant in Geothermal Power Plant Circulating Water. In: Proceedings of the World Geothermal Congress 2000. Kyushu-Tohoku, Japan. May-June 2000. pp. 3205-3209.

Li, M.F., Tang, X.P., Wu, W., and Liu, H.B. (2013). General models for estimating daily global solar radiation for different solar radiation zones in mainland China. Energy conversion and management, 70, 139-148.

Manceau, A., Ildefonse, P., Hazemann, J. L., Flank, A. M., and Gallup, D. (1995). Crystal chemistry of hydrous iron silicate scale deposits at the Salton Sea geothermal field. Clays and Clay Minerals, 43(3), 304-317.

Marshall, W. L., and Warakomski, J. M. (1980). Amorphous silica solubilities—II. Effect of aqueous salt solutions at 25 C. Geochimica et Cosmochimica Acta, 44(7), 915-924.

Mi, B., and Elimelech, M. (2013). Silica scaling and scaling reversibility in forward osmosis. Desalination, 312, 75-81.

Moraga, J., Duzgun, H.S., Cavur, M., and Soydan, H. (2022). The Geothermal Artificial Intelligence for geothermal exploration, Renewable Energy, 192, 134-149.

Relenyi, A. G., and Rosser Jr, H. R. (2019). Sulfur Deposit Removal and Control in A Power Plant Cooling Tower: A Case History from Cerro Prieto, Mexico’s Largest Geothermal Field. In: Proceedings of New Zealand Geothermal Workshop. Auckland, New Zealand.

Rodriguez, E. (2023). Online Cleaning of Direct Contact Condenser to Remove Sulfur Deposition. Geothermal Resources Council Transactions, 47, pp. 132-142.

Rothbaum, H.P., Anderton, B.H., Harrison, R.F., Rohde, A.G., and Slatter, A. (1979). Effect of silica polymerisation and pH on geothermal scaling. Geothermics, 8 (1), 1–20.

Shahdi, A., Lee, S., Karpatne, A., and Nojabaei, B. (2021). Exploratory analysis of machine learning methods in predicting subsurface temperature and geothermal gradient of Northeastern United States, Geothermal Energy, 9, 18.

Tarutani, T. (1989). Polymerization of silicic acid a review. Analytical sciences, 5(3), 245-252.

Wang, L., Yu, Z., Zhang, Y., and Yao, P. (2023). Review of machine learning methods applied to enhanced geothermal systems, Environmental Earth Sciences, 82(3), 69.

Wanner, C., Eichinger, F., Jahrfeld, T., and Diamond, L.W., (2017). Causes of abundant calcite scaling in geothermal wells in the Bavarian Molasse Basin, Southern Germany. Geothermics, 70, 324–338.

Yanaze, T., Yoo, S., Marumo, K., and Ueda, A., (2019). Prediction of permeability reduction due to silica scale deposition with a geochemical clogging model at Sumikawa Geothermal Power Plant. Geothermics, 79, 114–128.

Yokoyama, T., Sato, Y., Maeda, Y., Tarutani, T., and Itoi, R., (1993). Siliceous deposits formed from geothermal water I. The major constituents and the existing states of iron and aluminium. Geochemical Journal, 27 (6), 375–384.

Yokoyama, T., Takahashi, Y., Yamanaka, C., and Tarutani, T. (1989). Effect of aluminium on the polymerization silicic acid in aqueous solution and the deposition of silica of silica. Geothermics, 18(1-2), 321-326.